Yuzhen Jin*, **Shihe Zhu**, **Jingyu Cui**, **Jun Li**, **Zuchao Zhu**

Zhejiang Sci-Tech University,
Zhejiang Provincial Key Lab
of Modern Textile Machinery & Technology,
Xiasha Higher Educated Zone,
Hangzhou, Zhejiang Province 310018,
China
* E-mail: yzjin@zstu.edu.cn

Investigating the Effect of the Opening Unit on the Airflow Field in Rotor Spinning

DOI: 10.5604/01.3001.0010.4622

Abstract
The opening unit is an important device in a rotor spinning unit to comb fibres and remove trash. In this paper, numerical simulation is carried out to study the flow structure in the rotor spinning channel and the trash removal process in the trash removal unit. Firstly the effect of the opening unit on the airflow field in the rotor channel is investigated by single-phase simulation. The result shows that the effective area for fibre conveyance enlarges as the absolute value of negative pressure at the outlet increases, while it decreases as the opening roller speed increases. However, the effect of the negative pressure and the opening roller speed on the length of the vortex in the axial direction is quite small. Secondly the trash separation process in the trash removal unit is simulated using the Discrete Phase Model (DPM). Suitable rotational speeds of particles of different diameters are acquired. These results could provide a valuable reference for parameter selection in the trash-removal process.

Key words: *rotor spinning, opening unit, flow characteristics, trash removal, fibre opening, Discrete Phase Model (DPM).*

Introduction

As a kind of open-end spinning, rotor spinning is one of the new spinning technologies that have been industrialised. The rotor type open-end spinning machine mainly consists of a rotor, feed roller, opening unit, navel, and a delivery. Fibre combing is performed by the opening roller, in which slivers are fed from the fibre inlet. When fibres are fed into the fibre inlet, they are substantially combed into single fibre or a single fibre group by the opening roller, where teeth are uniformly distributed. These fibres finally enter the transfer channel by means of the centrifugal force of the opening roller and airflow. During the opening process, trashs are separated out by the trash removal unit. It is necessary to reduce the trash in the collecting groove of the rotor to improve the quality of the final product–yarn. For higher yarn's quality and better trash removal efficiency, it is necessary to conduct comprehensive research on the flow mechanism in the opening unit.

Some efforts have already been made to study the airflow characteristics, fibre configurations and yarn properties through experiments and simulations. Ripka and Junek et al. [1] established a simple model to compute the fibre flow. However, his model is too simple to take fibre gravity, buoyancy, and fibre configuration into consideration. Smith and Roberts [2] simulated fibre transport through a converging channel in a steady laminar fluid. However, their theoretical work on fibre configuration was limited. Lunenschloss, Coll-Tortosa and Siersch [3] applied infrared techniques to study fibre flow and fibre orientation in the fibre duct of an open-end rotor spinning machine. They found that a larger transfer channel inlet could make fibres accumulate and disorientate, and consequently deteriorate yarn properties. Lawrence and Chen [4, 5] studied fibre movement within a fibre transfer channel through experiment and observed that fibre configurations at the inlet region were different due to the variation in fibre length and manner of fibre detachment from the pins. Kong and Platfoot [6] established a simplified 2-D transfer channel model without considering the influence of the pins on the surface of the opening roller. They found that the distribution of stream lines does not vary dramatically with an increase in Reynolds numbers. Their results indicated that the speed of the opening roller could affect the flow structures greatly. In their further study [7], they found that the strong recirculation deteriorated the fibre's straightness, and consequently the yarn's quality. Due to the complex shape of the opening unit, they omitted the teeth of the opening roller to simulate the transfer channel by means of Computational Fluid Dynamic (CFD). Peyravi, Eskandarnejad and Moghadam [8] proposed a modified RU04 rotor spinning unit to improve yarn properties. They found that there is no significant difference between the extracted trash of dual-feed yarn and conventional yarns. It can be concluded that the changes in dimensions, shapes of the inlet of the transfer channel [4, 5], negative pressure at the outlet of the transfer channel [5, 9], and the opening roller's speed [10] would affect the rotor spun yarn's quality by changing the configuration of fibres. Based on their studies, a conventional opening unit with a single feed roller was utilised in this study.

Scholars have made some meaningful explorations of the flow characteristics in the opening unit. Their studies focused mainly on airflow patterns and their impact on the fibre configuration and yarn properties by means of experiments or simulation with a simplified model. A more practical geometric model of the opening roller which takes the teeth into consideration is used in this paper. The effect of the opening unit on the airflow field in the rotor spinning is investigated. Besides this, trash removal efficiency is also analysed. These results could provide a valuable reference for parameter selection in the trash removal process.

Model and mesh generation

Geometry model of trash removal device

A two-dimensional model for the trash removal device is constructed in this paper, which is shown in ***Figure 1***. The interface, which divides the rotational area into two parts, is defined to exchange data of different parts in the process of simulation. Line AB is set, which is perpendicular to the axis of the transfer channel and must go through point B.

Boundary condition and mesh generation

The fibre outlet is set as the pressure outlet in the simulation. The pressure inlet is applied to the fibre inlet, trash outlet and air inlet, the values of which are the same as for atmospheric pressure. The outlet pressure of the transfer channel, namely the fibre outlet pressure, is a negative value.

The mesh generated for the opening unit is shown in ***Figure 2***. As we can see, the computational domain consists of four different parts, including a transfer channel, trash area, inlet area and rotational area. To make the computation more efficient, hybrid mesh, which uses both structured and unstructured mesh, is adopted in this model for its flexibility and high efficiency. For this geometry, structured mesh is generated in the transfer channel and trash area. And the rest part is prepared with unstructured mesh to deal with the complex geometry. There are about 15.2 thousand mesh points in all.

Grid independence has been verified at conditions where the pressure at the inlet of the opening unit is 0 Pa, that at the outlet of the transfer channel -2000 Pa, and the opening roller speed 7000 r/min. The numbers of mesh used to check the grid independence are 15.2 thousand, 32.6 thousand, and 50.5 thousand, respectively. The static pressure at the monitoring point (26.49, 22.83) calculated with the three groups of mesh is shown in ***Table 1.*** It is found that the variation in the static pressure is less than 2%. Thus the grid used in this study is feasible, and it satisfies the requirement of grid independent solutions. Therefore the grid of 15.2 thousand we used for resolving the airflow field can meet the accuracy requirement.

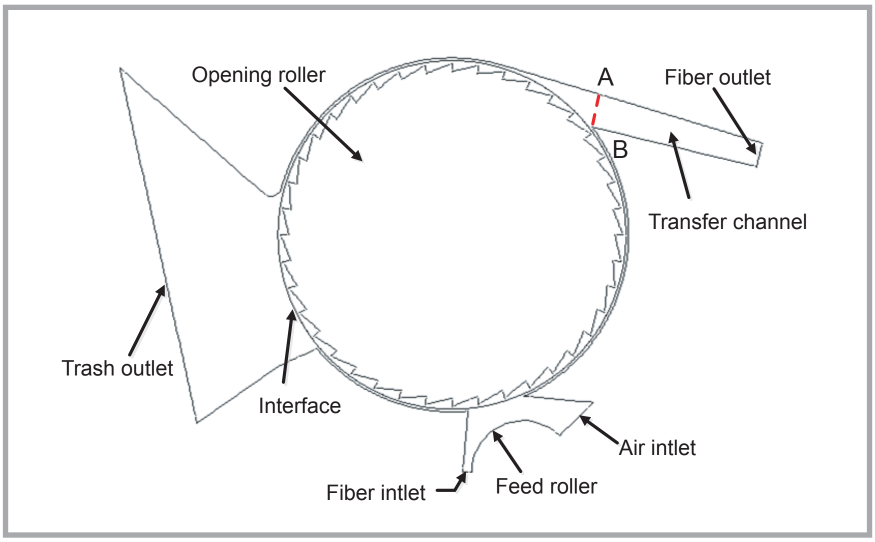

Figure 1. *Two-dimensional geometry model of the opening unit.*

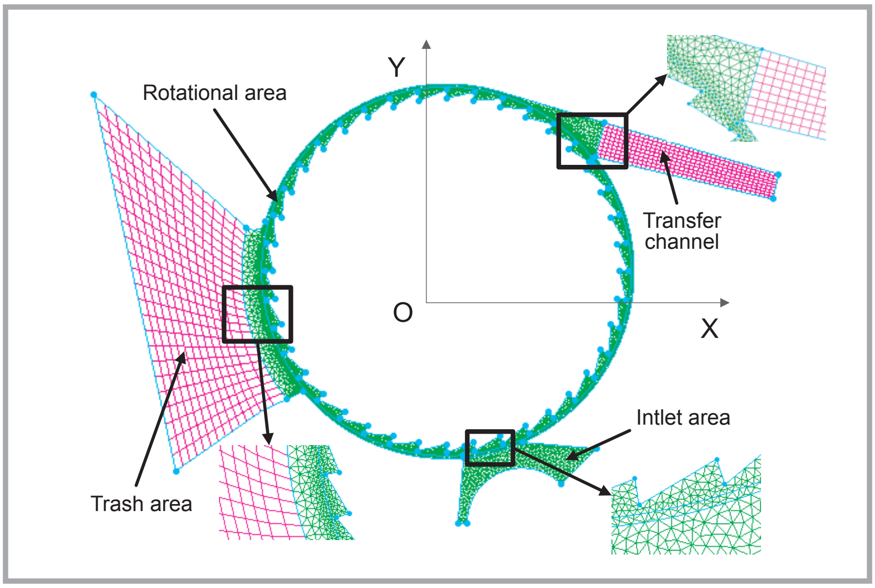

Figure 2. *Mesh generated for the opening unit model.*

Governing equations and algorithms

Continuity equation:

$$\frac{\partial(\rho u)}{\partial x}+\frac{\partial(\rho v)}{\partial y}+\frac{\partial(\rho w)}{\partial z}=0 \quad (1)$$

The N-S equations:

$$\begin{aligned}&\rho(\frac{\partial u}{\partial t}+u\frac{\partial u}{\partial x}+v\frac{\partial u}{\partial y}+w\frac{\partial u}{\partial z})=\\&=-\frac{\partial \rho}{\partial x}+\mu(\frac{\partial^2 u}{\partial x^2}+\frac{\partial^2 u}{\partial y^2}+\frac{\partial^2 u}{\partial z^2})+\rho g_x\end{aligned} \quad (2)$$

$$\begin{aligned}&\rho(\frac{\partial v}{\partial t}+u\frac{\partial v}{\partial x}+v\frac{\partial v}{\partial y}+w\frac{\partial v}{\partial z})=\\&=-\frac{\partial \rho}{\partial y}+\mu(\frac{\partial^2 v}{\partial x^2}+\frac{\partial^2 v}{\partial y^2}+\frac{\partial^2 v}{\partial z^2})+\rho g_y\end{aligned} \quad (3)$$

$$\begin{aligned}&\rho(\frac{\partial w}{\partial t}+u\frac{\partial w}{\partial x}+v\frac{\partial w}{\partial y}+w\frac{\partial w}{\partial z})=\\&=-\frac{\partial \rho}{\partial z}+\mu(\frac{\partial^2 w}{\partial x^2}+\frac{\partial^2 w}{\partial y^2}+\frac{\partial^2 w}{\partial z^2})+\rho g_z\end{aligned} \quad (4)$$

Moving reference frames (MRF) are selected to consider the effect of the teeth of the opening roller on the flow field. This method is suitabe for the condition where the relative motion of each point on the mesh boundary is roughly the same.

Consider a coordinate system that translates with a linear velocity $\vec{v}_t$ and rotates with an angular velocity $\vec{\omega}$ relative to the stationary (inertial) reference frame.

The axis of rotation is defined by a unit direction vector $\hat{a}$ such that

$$\vec{\omega}=\omega\hat{a} \quad (5)$$

The computational domain for the CFD problem is defined with respect to the moving frame such that an arbitrary point in the CFD domain is located by a position vector $\vec{r}$ from the origin of the moving frame.

Table 1. *Check of grid independence.*

Grid number	Static pressure, Pa	Velocity magnitude, m/s
15.2 thousand	-1991.70	9.3
32.6 thousand	-1957.14	9.35
50.5 thousand	-1959.99	9.46

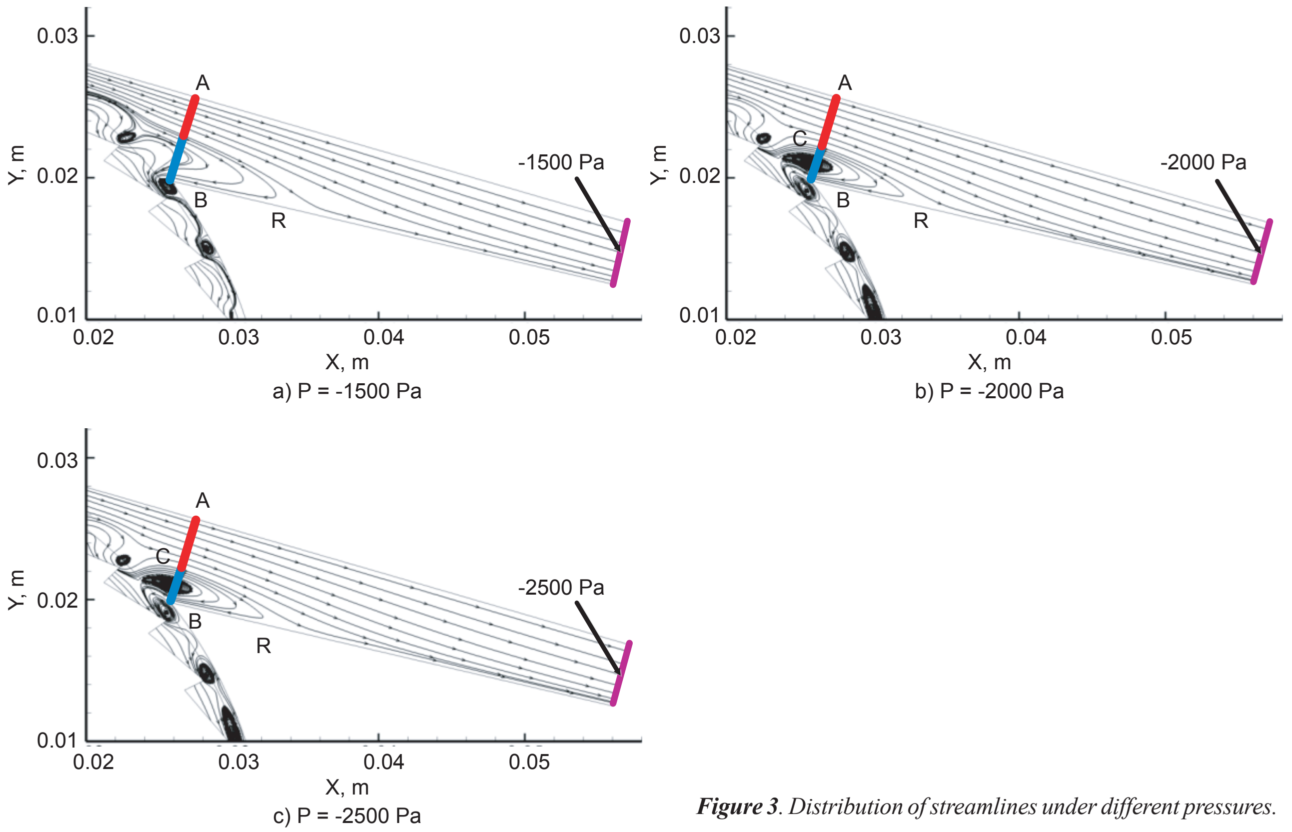

***Figure 3**. Distribution of streamlines under different pressures.*

The fluid velocity can be transformed from the stationary frame to the moving frame using the following formula:

$$\vec{v}_r = \vec{v} - \vec{u}_r \qquad (6)$$

Where

$$\vec{u}_r = \vec{v}_t + \vec{\omega} \times \vec{r} \qquad (7)$$

$\vec{v}_r$ is the relative velocity, $\vec{v}$ is the absolute velocity, $\vec{u}_r$ is the velocity of the moving frame relative to the inertial reference, $\vec{v}_t$ is the translational frame velocity, and $\hat{\omega}$ is the angular velocity. It should be noted that $\hat{\omega}$ and $\vec{v}_t$ are functions of time.

For absolute velocity formulation, the governing equations of fluid for a steadily moving frame can be written as follows:

Conservation of mass:

$$\frac{\partial \rho}{\partial t} + \nabla \cdot \rho \vec{v}_r = 0 \qquad (8)$$

Conservation of momentum:

$$\frac{\partial}{\partial t}\rho\vec{v} + \nabla \cdot (\rho \vec{v}_r \vec{v}) + \rho[\vec{\omega} \times (\vec{v} - \vec{v}_t)] = -\nabla \mathrm{p} + \nabla \cdot \bar{\tau} + \vec{F} \qquad (9)$$

Conservation of energy:

$$\frac{\partial}{\partial t}\rho E + \nabla \cdot (\rho \vec{v}_r H + p \vec{u}_r) = \nabla \cdot (k \nabla T + \bar{\tau} \cdot \vec{v}) + S_h \qquad (10)$$

Where $\bar{\tau}$ is the viscous stress, E is the internal energy, and H is the total enthalpy. The standard $k-\varepsilon$ (2 equations) model is adopted to resolve the turbulent flow and cooperate with MRF.

In addition, the Discrete Phase Model (DPM) is applied to the simulation of particle trajectories. The force balance in DPM can be written as:

$$\frac{d\vec{u}_p}{dt} = \frac{\vec{u} - \vec{u}_p}{\tau_r} + \frac{\vec{g}(\rho_p - \rho)}{\rho_p} + \vec{F} \qquad (11)$$

Where $\vec{F}$ is an additional acceleration (force/unit particle mass) term, $\frac{\vec{u} - \vec{u}_p}{\tau_r}$ is the drag force per unit particle mass, and τ_r is the droplet or particle relaxation time, the formula is shown as follows:

$$\tau_r = \frac{p_p d_p^{\,2}}{18\mu} \frac{24}{C_d \,\mathrm{Re}} \qquad (12)$$

$\vec{u}$ is the fluid phase velocity, $\vec{u}_p$ is the particle velocity, u the molecular viscosity of fluid, ρ is the fluid density, ρ_p is the density of the particle, and d_p is the particle diameter. Re is the relative Reynolds number, which is defined as

$$\mathrm{Re} \equiv \frac{\rho d_p |\vec{u}_p - \vec{u}|}{\mu} \qquad (13)$$

The finite volume method (FVM) is used to discretise the governing equations. The semi-implicit method for the pressure linked equation (SIMPLE) algorithm is employed to iterate the system of equations. The convergence criterion is defined as the relative residual being less than 10^{-3} for each variable. The density of air is 1.225 kg/m^3 and its viscosity is 1.7894×10^{-5}Pa s. The pressure-based steady algorithm is used in this solver.

Numerical simulation and analysis

Simulation of the airflow field in the transfer channel

The transfer channel is the last part before fibres enter the rotor. The airflow in the transfer channel has a great impact on fibre configurations and yarn properties. Therefore streamlines and velocity corresponding to different outlet pressures are studied in this paper. The pressure of the fibre outlet is set as -1500 Pa, -2000 Pa and -2500 Pa, respectively. The working speed of the opening roller is generally between 5000 rpm and 9000 rpm. It is found that the yarn tenacity and elongation decrease significantly as the opening

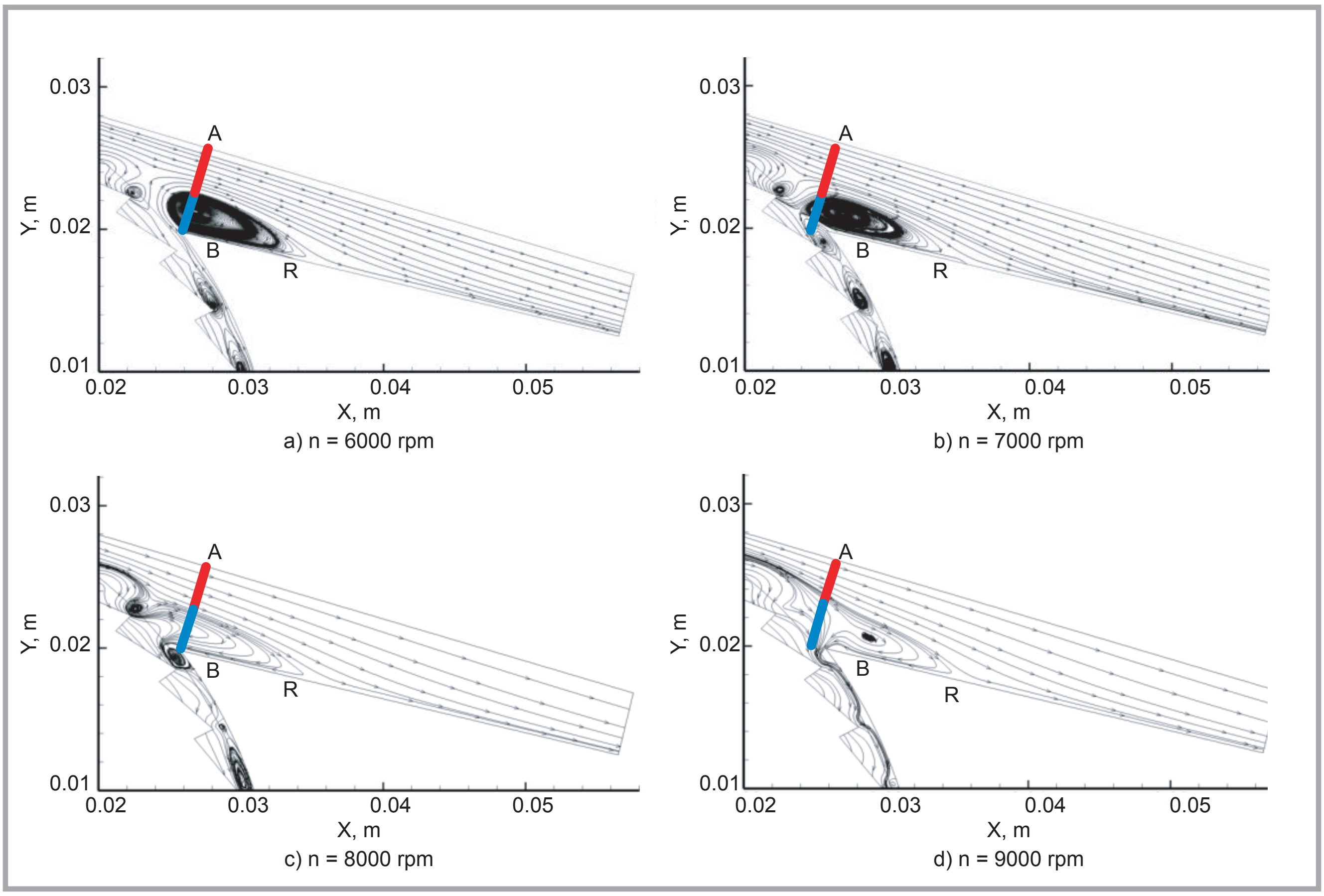

***Figure 4**. Distributions of streamlines under different rotational speeds*

roller speed increases, while yarn imperfections gradually decrease with an increase in the opening roller speed. In order to balance yarn imperfections and yarn tenacity, the opening roller speed here is set as 7000 rpm. The airflow near the opening roller in the transfer channel, namely the vortex zone, is particularly investigated in this research.

The streamlines in the transfer channel corresponding to different pressures are shown in ***Figure 3***. A negative pressure value at the outlet of the transfer channel has an apparent impact on the streamlines. When the pressure is -1500 Pa, streamlines at the junction of the opening roller and transfer channel change their original directions and turn to opposite directions. When the pressure is -2000 Pa, a small vortex forms at the junction of the opening roller and transfer channel. When the pressure is -2500 Pa, streamlines near the bottom of the transfer channel develop into a relatively strong and large vortex.

As the negative pressure value increases, streamlines situated at the junction of the opening roller and transfer channel gradually form a vortex, which has a negative impact on the fibre because it makes the fibre easy to buckle and deform. The reattachment point , defined as the point of the flow shear layer, almost ends in the same position. The length of the vortex in the axis direction of the transfer channel does not change in general when the negative pressure changes from -1500 Pa to -2500 Pa. However, the size of the vortex in the direction perpendicular to the axis of the channel decreases, which means that the effective width [6] in this direction increases. The effective width is defined as the width of a cross section containing forward moving flow and is marked by a red line in ***Figure 3***. The ratio of the vortex width to the geometric width in ***Figure 3*** is about 50.7%, 39.1% and 40.5%, respectively. The ratio of effective width to geometric width is 49.3%, 60.9% and 59.5%, respectively. Subsequently the effective area for fibre conveyance without collision could enlarge as the outlet pressure changes from -1500 Pa to -2000 Pa. When the pressure decreases to -2000 Pa, the effective area for fibre conveyance is basically unchanged.

In summary, the greater the negative pressure value of the fibre outlet is, the greater the intensity of the vortex is. However, the effective width enlarges with an increase in the negative pressure value. The effective area for fibre conveyance enlarges with an increase in the absolute value of negative pressure at the outlet of the transfer channel. A great negative pressure value is conducive to fibre transmission.

The rotational opening roller speed is set as 6000 rpm, 7000 rpm, 8000 rpm and 9000 rpm, respectively. The fibre outlet pressure is set as -2000 Pa. Distributions of streamlines at different rotational speeds are shown in ***Figure 4***. When the rotational speed is between 6000 rpm and 7000 rpm, there is a vortex at the bottom of the transfer channel. And when the rotational speed increases from 8000 rpm to 9000 rpm, the enclosed area of streamlines almost disappears. Although rotational speeds of the opening roller are different, the vortex almost ends in the same position; namely, the reattachment point is almost located in the same place. Consequently the rotational speed has little impact on the length of the vortex in the axis direction of the channel. The ratio of the vortex width to the geometric

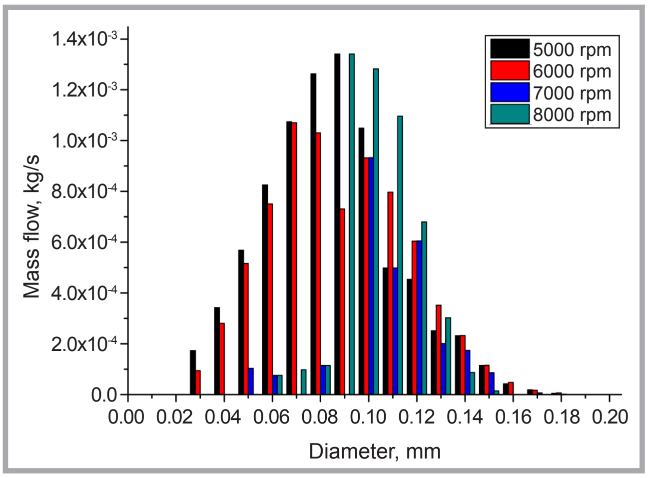

***Figure 5**. Mass flow of different particles passing through the trash outlet.*

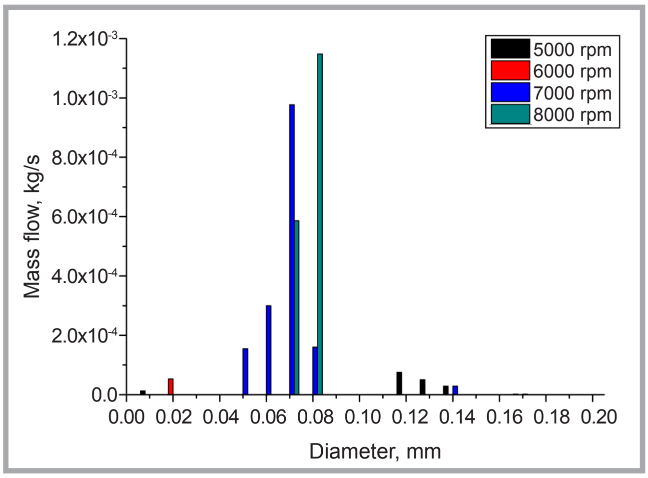

***Figure 6**. Mass flow of different particles passing through the fibre outlet.*

width in ***Figure 4*** is about 46.4%, 43.5%, 47.8% and 52.2%, respectively, and the ratio of the effective width to the geometric width is 53.6%, 56.5%, 52.2% and 47.8% respectively. It means that the effective width for fibre conveyance decreases. Subsequently the effective area for fibre conveyance decreases with an increase in the rotational opening roller speed. In order to reduce the negative impact of the vortex, the rotational speed should not be higher than 8000 rpm.

Simulation of trash removal

The discrete phase model (DPM) is used to simulate the trash removal process in the opening roller. The boundary conditions of the trash outlet, fibre outlet, fibre inlet and air inlet for DPM are set as the escape boundary condition. The reflect type is selected to be the boundary condition for those walls. According to statistics from numerical simulation, suitable rotational speeds of the opening roller corresponding to particles of different diameters are explored.

According to the studies of Murugan [11] and Ishtiaque [12], the speed of the opening roller is invariably related to the trash removal. If the opening roller speed is low, fibres and trash are poorly separated. Higher opening roller speeds will result in many broken fibres during separation. The speed of the opening roller is chosen as 5000 rpm, 6000 rpm, 7000 rpm and 8000 rpm respectively. Parameters for DPM calculation are listed in ***Table 2***. In addition, the mean diameter of these particles is set as 0.10 mm. The mass flow of different particles released from the fibre inlet follow the law of normal distribution.

__Table 2__. Parameter settings.

Parameter settings	
Fibre outlet pressure, Pa	−2000
Diameters of trash particles, mm	0.01~0.20
Total mass flow, kg/s	0.01
initial speed of trash particles, m/s	0.05

The mass flow of different particles passing through the trash outlet and fibre outlet are shown in ***Figure 5*** and ***Figure 6***, respectively. The mass flow of different particles in ***Figure 5*** follows the law of normal distribution in general. Comparing the mass flow of different particles at different speeds, 5000~6000 rpm of the opening roller is beneficial to the removal of trash particles whose diameters are between 0.03 mm and 0.09 mm according to simulation results. Particles at the speed of 8000 rpm mainly distribute in the range of 0.09~0.13 mm. ***Figure 6*** shows the mass flow of different particles passing through the fibre outlet, suggesting that a rotational speed of 5000~6000 rpm for the opening roller is not preferable for trash particles whose diameter is 0.01~0.02 mm or 0.12~0.14 mm. Moreover 7000~8000 rpm of the opening roller is not suitable for trash particles whose diameter is smaller than 0.09 mm.

The ratio of mass flow passing through the trash outlet to the total mass flow shows the effective efficiency of trash removal. ***Table 3*** shows the mass flow of particles passing through different inlets and outlets at varios opening roller speeds. It can be seen that the trash removal efficiency declines from 82.5% to 50.9% with an increase in the opening roller speed. The minimum mass flow passing through trash outlet accounts for 50.9% of the total mass flow. Apart from the speed of 6000 rpm, the ratio of mass flow passing through the fibre outlet to the total mass flow increases from 1.7% to 17.3% simultaneously. It can be concluded that different opening roller speeds have different removal efficiency for different sizes of trash particles.

From ***Table 3***, it can be seen that a considerable number of particles escape from the fibre inlet, especially particles at the speed of 7000 rpm and 8000 rpm. The ratio of mass flow passing through the fibre inlet to the total mass flow at each rotational speed is 9.4%, 20.8%, 32.5% and 31.7%, respectively. This means that these particles escape from the opening unit without trash removal.

Figure 7 shows the distribution of streamlines near the inlet at different speeds. When the speed is between 5000 rpm and 6000 rpm, the major vortex occupies the entire channel on the upper part. While the speed is between 7000 rpm and 8000 rpm, the vortex is closer to the feed roller, occupying a part of the channel. With an increase in the opening roller speed, the effect of the opening roller on the airflow field near the inlet is more significant.

Conslusions

The effect of the opening unit on the airflow field in rotor spinning is investigated by establishing a practical geometry model of the opening unit. The con-

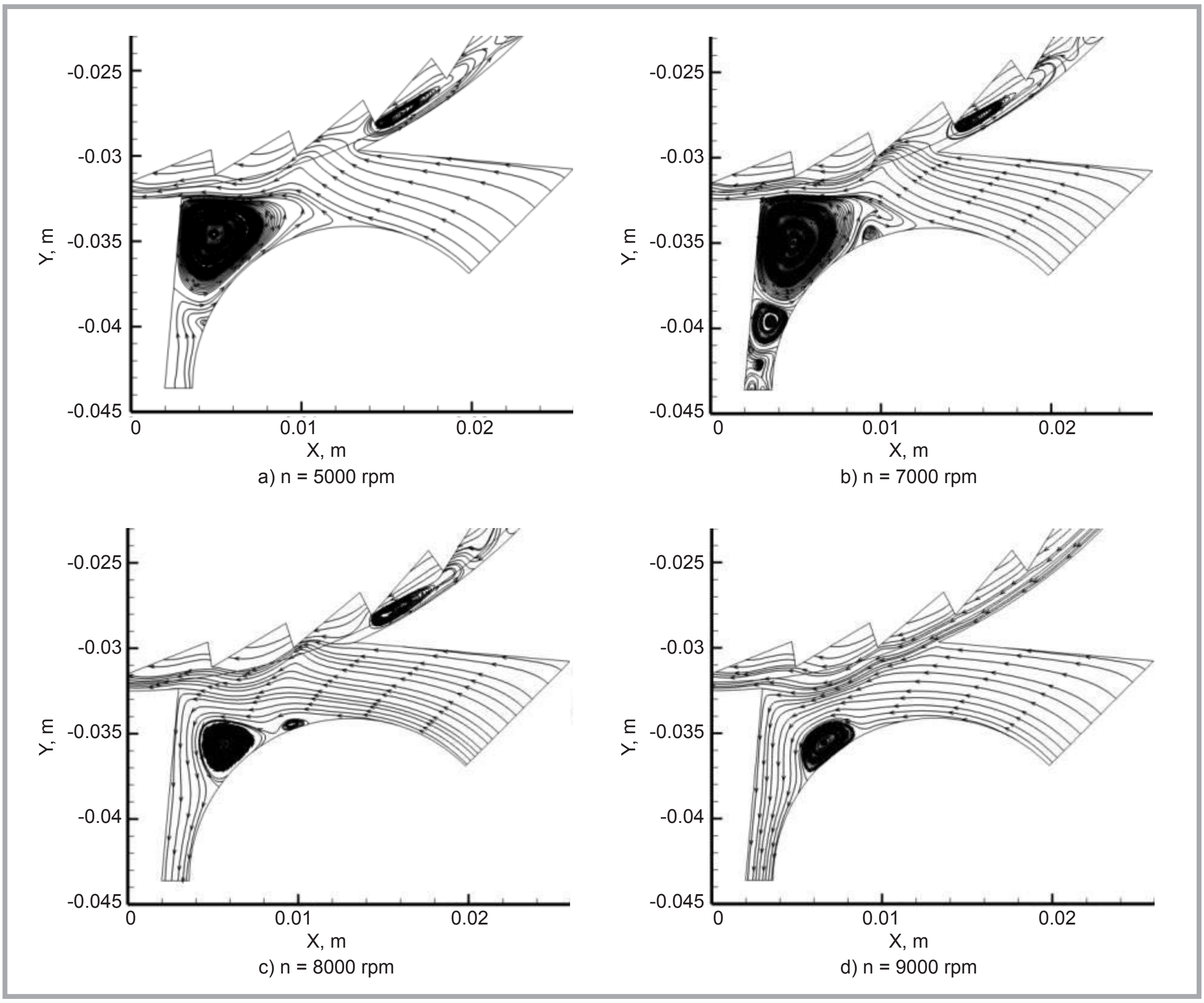

***Figure** 7. Distribution of streamlines near the inlet for different speeds.*

clusions deduced from the discussions above are summarised as follows:

1. The opening roller speed and negative pressure at the outlet have little impact on the length of the vortex in the axial direction. The effective area for fibre conveyance enlarges as the absolute value of negative pressure at the outlet of the transfer channel increases, while it decrease as the opening roller speed increases. A greater pressure value is conducive to fibre transmission. A higher opening roller speed is detrimental to the fibre configuration. In order to reduce the negative impact of the vortex, the opening roller speed should not be higher than 8000 rpm in the fibre-transfer process.
2. A relatively low opening roller speed is suitable for removing trash particles of smaller diameters, and a relatively high opening roller speed is suitable for removing trash particles of larger diameters.
3. Different opening roller speeds have different removal efficiency for variuos sizes of the trash particle. A rotational speed of 5000~6000 rpm for the opening roller is not preferable for trash particles whose diameter is 0.01~0.02 mm or 0.12~0.14 mm, while 7000~8000 rpm of the opening roller is not suitable for particles whose diameter is smaller than 0.09 mm.

***Table 3**. Mass flow of particles passing through different inlet/outlets at various opening roller speeds.*

Opening roller speed, rpm	Trash outlet		Fibre outlet		Fibre inlet		Sum	
	Mass flow, kg/s	Percentage, %	Mass flow, kg/s	Percentage, %	Mass flow, kg/s	Percentage, %	Mass flow, kg/s	Percentage, %
5000	8.25E-3	82.5	1.70E-4	1.7	9.38E-4	9.4	9.36E-3	93.6
6000	7.58E-3	75.8	5.30E-5	0.5	2.08E-3	20.8	9.70E-3	97.0
7000	5.96E-3	59.6	7.68E-4	7.68	3.25E-3	32.5	9.97E-3	99.7
8000	5.09E-3	50.9	1.73E-3	17.3	3.18E-3	31.7	9.90E-3	99.9

Acknowledgements

The work was supported by National Natural Science Foundation of China under Grant No.51576180, Zhejiang Provincial Natural Science Foundation under Grant No.LZ14E050004, and Project of 521 Talents Cultivation in Zhejiang Sci-Tech University.

References

1. Ripka J, Junek J. Trajectory of Fiber Conveyed from the Combing-out Cylinder Clothing into a Parallel Air Zone (in Czech). *Textile* 1975; 30 (4), 125-129.
2. Smith AC, Roberts WW. Straightening of Crimped and Hooked Fibers in Converging Transport Ducts: Computational Modelling. *Textile Research Journal* 1994; 64(6), 335-344.
3. Lunenschloss J, Coll-Tortosa L, Siersch E. Fiber Flow and Fiber Orientation in the Fiber Duct of an O.E. rotor Spinning Machine. *Chemiefasern/Textilindustrie* 1976; 26(78), 165-169.
4. Lawrence CA, Chen KZ. A Study of the Fiber transfer-channel Design in Rotor-spinning, Part I: The Fiber Trajectory. *The Journal of the Textile Institute* 1988; 79 (3), 367-392.
5. Lawrence CA; Chen KZ. A Study of the Fiber transfer-channel Design in Rotor-spinning, Part II: Optimisation of the Transfer-channel Design. *The Journal of the Textile Institute* 1988; 79(3), 393-408.
6. Kong LX, Platfoot RA. Two-Dimensional Simulation of Air Flow in the Transfer Channel of Open End Rotor Spinning Machines. *Textile Research Journal* 1996; 66 (10), 641-650.
7. Kong LX, Platfoot RA. Fibre transportation in confined channel with recirculation. *Computers and Structures* 2000; 78, 237-245.
8. Peyravi A, Eskandarnejad S, Moghadam MB. Dual-feed rotor spinning of cotton fiber: trash separation and yarn properties. *The Journal of the Textile Institute* 2014; 105(4), 377-382.
9. Polyanskii YB, Mayanskii SE. Study on the effect of the dimensions of the fibre transport channel and the rotor vacuum in an open-end spinning machine on yarn quality. *Tekhnologiya Tekstil'noi Promyshl-ennosh* 1992; 4: 25-28.
10. Kong LX, Platfoot RA, Wang X. Effects of Fiber Opening on the uniformity of Rotor Spun Yarns. *Textile Research Journal* 1996; 66 (1), 30-36.
11. Murugan R, Dasaradan BS, Karnan P, Senthilkannan MS. Fibre Rupture Phenomenon in Rotor Spinning. *Fibers and Polymers* 2007; 8(6), 665-668.
12. Ishtiaque SM. Longitudinal Fiber Distribution in Relation to Rotor Spun Yarn Properties. *Textile Research Journal* 1989; 59, 696-699.

Received 20.10.2016 Reviewed 15.03.2017